Received: 24 November 2019 | Revised: 24 February 2020 | Accepted: 9 March 2020

DOI: 10.1002/ajmg.a.61570

ORIGINAL ARTICLE

AMERICAN JOURNAL OF medical genetics PART A WILEY

Human *RAD50* deficiency: Confirmation of a distinctive phenotype

Aviël Ragamin[1] | Gökhan Yigit[2] | Kristine Bousset[3] | Filippo Beleggia[4] | Frans W. Verheijen[1] | Marie-Claire Y. de Wit[5,6] | Tim M. Strom[7,8] | Thilo Dörk[3] | Bernd Wollnik[2,9] | Grazia M. S. Mancini[1,6]

[1]Department of Clinical Genetics, Erasmus MC University Medical Center, Rotterdam, The Netherlands

[2]Institute of Human Genetics, University Medical Center Göttingen, Göttingen, Germany

[3]Department of Gynecology and Obstetrics, Hannover Medical School, Hannover, Germany

[4]Clinic I of Internal Medicine, University Hospital Cologne, Cologne, Germany

[5]Department of Child Neurology, Sophia Children's Hospital, Erasmus MC University Medical Center, Rotterdam, Netherlands

[6]ENCORE Expertise Center for Neurodevelopmental Disorders, Rotterdam, The Netherlands

[7]Institute of Human Genetics, Helmholtz Zentrum München, Neuherberg, Germany

[8]Institute of Human Genetics, Technische Universität München, Munich, Germany

[9]Cluster of Excellence "Multiscale Bioimaging: From Molecular Machines to Networks of Excitable Cells" (MBExC), University of Göttingen, Göttingen, Germany

Correspondence
Grazia M. S. Mancini, Department of Clinical Genetics, Erasmus Medical Center, Rotterdam, The Netherlands.
Email: g.mancini@erasmusmc.nl

Funding information
ZonMw, Grant/Award Number: 91217045

Abstract

DNA double-strand breaks (DSBs) are highly toxic DNA lesions that can lead to chromosomal instability, loss of genes and cancer. The MRE11/RAD50/NBN (MRN) complex is keystone involved in signaling processes inducing the repair of DSB by, for example, in activating pathways leading to homologous recombination repair and nonhomologous end joining. Additionally, the MRN complex also plays an important role in the maintenance of telomeres and can act as a stabilizer at replication forks. Mutations in *NBN* and *MRE11* are associated with Nijmegen breakage syndrome (NBS) and ataxia telangiectasia (AT)-like disorder, respectively. So far, only one single patient with biallelic loss of function variants in *RAD50* has been reported presenting with features classified as NBS-like disorder. Here, we report a long-term follow-up of an unrelated patient with facial dysmorphisms, microcephaly, skeletal features, and short stature who is homozygous for a novel variant in *RAD50*. We could show that this variant, c.2524G > A in exon 15 of the *RAD50* gene, induces aberrant splicing of *RAD50* mRNA mainly leading to premature protein truncation and thereby, most likely, to loss of RAD50 function. Using patient-derived primary fibroblasts, we could show abnormal radioresistant DNA synthesis confirming pathogenicity of the identified variant. Immunoblotting experiments showed strongly reduced protein levels of RAD50 in the patient-derived fibroblasts and provided evidence for a markedly reduced radiation-induced AT-mutated signaling. Comparison with the previously reported case and with patients presenting with NBS confirms that *RAD50* mutations lead to a similar, but distinctive phenotype.

KEYWORDS

DNA repair, microcephaly, MRN complex, Nijmegen breakage syndrome-like disorder, RAD50

1 | INTRODUCTION

Damage to DNA can result in a variety of chemical changes, ranging from base mismatches to double-strand breaks (DSBs) (Chatterjee &

Aviël Ragamin and Gökhan Yigit contributed equally to this study.

Walker, 2017). DSBs in particular can lead to loss of genes, chromosomal instability, and cancer (Aparicio, Baer, & Gautier, 2014). DSBs are toxic lesions that occur as a result of, for example, ionizing radiation or mishaps at the replication fork (Mehta & Haber, 2014). To repair DSBs and restore genomic integrity, eukaryotic cells have developed two major pathways: homologous recombination repair (HRR) and nonhomologous end joining (NHEJ). The MRE11A/RAD50/NBN (MRN) complex is involved in both, HRR and NHEJ (Hoa et al., 2016; Kobayashi, Antoccia, Tauchi, Matsuura, & Komatsu, 2004; Yang et al., 2006). It consists of highly conserved proteins of which MRE11A and RAD50 can be found even in lower eukaryotes such as yeasts (Chamankhah & Xiao, 1999). The importance of the MRN complex is highlighted by the fact that null mutations are incompatible with life in mice, and deficiency leads to severe defects in the ability to repair DNA (Luo et al., 1999; Xiao & Weaver, 1997; Zhu, Petersen, Tessarollo, & Nussenzweig, 2001). The MRN complex has a cornerstone function in DSB-induced signaling as it interacts with ataxia telangiectasia-mutated (ATM) protein and thereby can activate pathways leading to HRR, NHEJ, and microhomology-mediated end joining. Additionally, the MRN complex also plays a role in the maintenance of the telomeres and acts as a stabilizer at replication forks (Lavin, Kozlov, Gatei, & Kijas, 2015; Stingele, Bellelli, & Boulton, 2017; Williams, Lees-Miller, & Tainer, 2010).

So far, mutations in all three components of the MRN complex have been reported in humans. Mutations in the *NBN* (*NBS1*) gene are associated with Nijmegen breakage syndrome (NBS, OMIM #251260), a disorder characterized by progressive microcephaly, mild to moderate short stature, dysmorphic facial features including a prominent nasal bridge and nose, sloping forehead, large ears, and retrognathia. Furthermore, patients with NBS present with premature ovarian insufficiency, immunodeficiency with recurrent pulmonary infections and increased risk of malignancies within the second decade of life. On a cellular level, chromosomal instability mostly involving Chromosomes 7 and 14, and abnormal radioresistant DNA synthesis of cultured cells can be observed (Chrzanowska et al., 1995; Varon, Demuth, & Chrzanowska, 1993).

Mutations in *MRE11A* have been identified in patients with an ataxia-telangiectasia-like disorder (ATLD Type 1, OMIM #604391). These present with progressive cerebellar ataxia, atrophy of cerebellar vermis and hemispheres, abnormal eye movements (oculomotor apraxia), and dysarthria as key features (Delia et al., 2004; Fernet et al., 2005; Fievet et al., 2019; Palmeri et al., 2013; Stewart et al., 1999). Abnormal radiosensitivity of cell cultures has been reported. In contrast to ataxia-telangiectasia (AT, OMIM #208900), patients with ATLD have no telangiectasia, no myelodysplasia and have normal immunoglobulin levels.

So far, only one patient with biallelic mutation in *RAD50* has been reported presenting with clinical features that partly resemble both, NBS and ATLD (Barbi et al., 1991; Waltes et al., 2009), OMIM #613078. Waltes et al. described a 23-year-old woman with compound heterozygosity for mutations in *RAD50* leading to a RAD50 protein deficiency. She showed dysmorphic facial features similar to NBS, short stature, microcephaly, and mild/moderate intellectual disability. Fibroblasts established from this patient showed chromosomal instability and abnormal radioresistant DNA synthesis. However, unlike NBS, this patient never developed severe infections. She had normal immunoglobulin levels and no malignancies were reported. Waltes et al. classified this disorder as a NBS-like disorder. In this study, we describe a long-term follow-up of a second patient with homozygosity for a novel *RAD50* variant, and we show pathogenicity of the identified variant and characterize the distinctive clinical phenotype of patients with *RAD50* mutations.

2 | METHODS

2.1 | Genetic analysis

G-banded chromosome analysis was performed according to routine standard procedures and genomic arrays were performed as previously described (van Zutven et al., 2018). DNA was isolated by standard procedures from blood leukocytes. Nucleotides were numbered according to the Human Genome Variation Society guidelines. We performed whole-exome sequencing (WES) on DNA extracted from blood lymphocytes of the affected index patient using the Agilent Sure Select Human All Exon 50 Mb enrichment kit. WES data analysis and filtering of variants were carried out as previously described (Bogershausen et al., 2015). RT-PCR was performed as described by Vandervore et al. (2019).

2.2 | Radioresistant DNA synthesis

Fibroblasts from our patient, a patient with AT and a control patient were isolated and DNA synthesis was measured as reported by de Wit, Jaspers, and Bootsma (1981). In short, cells were prelabeled with thymidine [^{14}C] and irradiated with γ-radiation at 5, 10, 15, and 20 Gy and then labeled with thymidine [^{3}H]. An ice-cold phosphate buffered saline was used to stop incubation. The ratio between ^{3}H and ^{14}C was used as a measure of DNA syntheses. DNA synthesis of unirradiated cells was used as baseline.

2.3 | Immunoblotting

Skin fibroblasts from our new patient (F583) were tested for their protein expression of RAD50 by immunoblotting following a lysis protocol previously described (Waltes et al., 2009) and compared with large-T immortalized fibroblast lines from the previously reported patient with RAD50 deficiency (F239-T) and from a healthy control (ADD-T) (Schroder-Heurich, Wieland, Lavin, Schindler, & Dork, 2014). Protein extracts were separated through SDS-PAGE followed by immunoblotting. The antibodies used were RAD50 (mouse monoclonal, Abcam, 1:500); MRE11A (mouse monoclonal 12D7, GeneTex, 1:1,000); NBN (rabbit polyclonal NB100-143, Novus, 1:5,000); and β-actin (mouse monoclonal AC15, Sigma, 1:3,000). To assess the

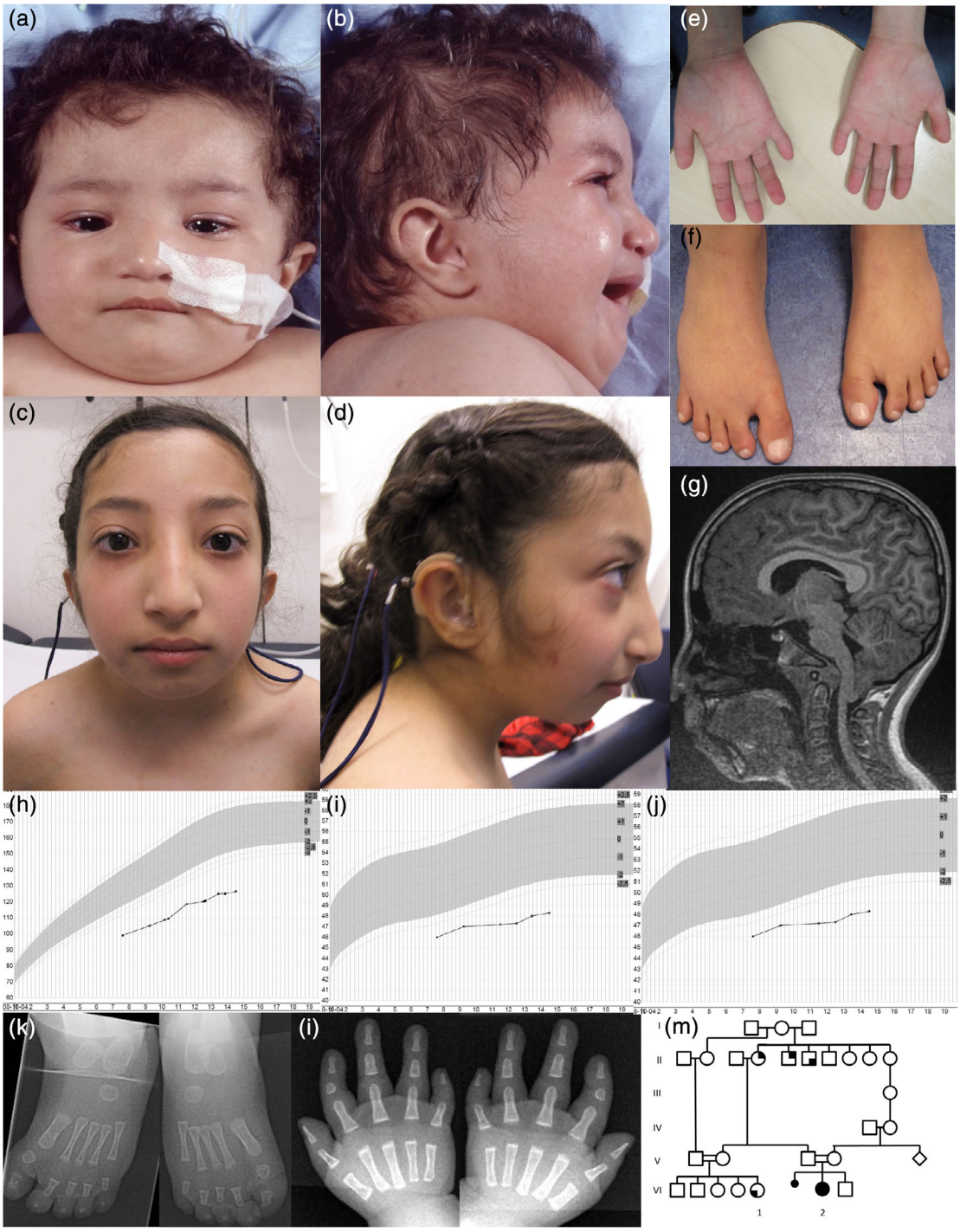

FIGURE 1 Clinical phenotype and pedigree. (a–d) Photographs of the facial features of the index patient at 10 months and 10 years old. Dysmorphic features at 10 months include a broad nose with depressed nasal bridge, hypertelorism, mild upslant of eyelids, a small lower lip, micrognathia, low implanted and rotated ears, and a short neck. At 10 years her features slightly changed, she had a prominent nose bridge with a long nose point and a sloping forehead. (e,f) Photographs from hands and feet show bilateral clinodactyly of the fingers and toes, bilateral transverse palmar crease, bilateral brachydactyly and a sandal gap. (g) Midsagittal T1 weighted images show normal development of midline brain structures, including corpus callosum, pituitary stalk, gyration, and cerebellum. The cerebellar tonsils, however, show herniation in the foramen magnum (Chiari malformation) and the medulla shows a (swan neck-like) kink associated by an abnormal position and morphology of the C2 vertebra. Signal intensity of the medulla and spinal cord are normal. (h–j) Growth data of the index patient. Weight (h), length (i), and occipitofrontal circumference (j) all below −2 *SD*. (k, l) Hand and feet X-rays of the index patient at 6 months old. X-rays of the hands show short mild phalanges of all digits and short phalanges of the first digits on both hands. X-rays of the feet shows short proximal phalanges of the first digits of both feet (Type A1 brachydactyly of Bell). In addition, the middle phalanges of the fifth digits on both hands are missing. (m) Family pedigree. Our proband is VI-2. Filled symbols indicate homozygosity for RAD50 mutation; left lower quadrant filled symbols indicate Seckel disease (proband's niece, VI-1); right upper quadrant filled symbols indicate colon carcinoma and right lower quadrant filled symbol indicates lung carcinoma [Color figure can be viewed at wileyonlinelibrary.com]

cellular ability of radiation-induced damage recognition and ATM activation, we irradiated the fibroblasts with 6 Gy using a Mevatron MD-2 accelerator (Siemens, Munich, Germany). Whole cell lysates were extracted at 30 min after irradiation and immunoblotting was performed against two targets of the ATM kinase, CHEK2(pSer19), and KAP1(pSer824) as previously described (Pietrucha et al., 2017). The antibodies used were pSer19-CHEK2 (rabbit polyclonal, Cell Signaling, 1:500) and pSer824-KAP1 (rabbit polyclonal, Bethyl Laboratories, 1:5,000). Anti-mouse and anti-rabbit horseradish peroxidases labeled secondary antibodies were purchased from GE Healthcare. Enhanced chemiluminescence (Dura ECL, Thermo Scientific/Pierce) was used for visualization of immunoreactive bands.

2.4 | Editorial policies, ethical considerations, and data availability statement

This study was conducted in accordance to the Helsinki Declaration and was approved by the ethics committee of the University of Cologne, Germany, and the ethics committee of the University Medical Center Göttingen, Germany. Informed written consent for reviewing medical records and publication of pictures was obtained from our proband and her parents. The data that support the findings of this study, including the RT-PCR primer sequences, are available upon request. The genomic data are not publicly available due to privacy restrictions.

3 | RESULTS

3.1 | Clinical report

The index patient, a 15-year-old female, was born as the first child of consanguineous Turkish parents. The family history refers that the paternal aunt, who was married to a fourth degree relative, had a daughter diagnosed with Seckel syndrome and presenting with growth delay. No medical record of this girl could be retrieved, however, pictures made available by the family show overlapping facial features to our index patient. During pregnancy, intrauterine growth retardation was recorded. The girl was born at 37 weeks of gestation with a birth weight of 1,520 g (−3.5 *SD*) and a head circumference of 29.5 cm (−3.5 *SD*). At birth, dysmorphic features were noted. Physical examination at 10 months of age revealed a broad nose with depressed nasal bridge, hypertelorism, mild upslanting eyelids with epicanthus inversus, a small lower lip, micrognathia, low implanted and rotated ears, a short neck, wide spaced nipples, bilateral clinodactyly of fingers and toes, bilateral transverse palmar crease, bilateral brachydactyly, a sandal gap, multiple café-au-lait macules, and high pitched cry (Figure 1a–f). Neonatal screening revealed hypothyroidism due to transient hypothyroxinemia as a result of dysmaturity. A normal female type karyotype was reported with no evidence for spontaneous chromosomal breakages. Metabolic and infectious screenings were normal. Her growth parameters remained below the −3 *SD* during her first year of age and she had feeding difficulties and gastroesophageal reflux. X-rays of hands and feet at the age of 6 months and a complete skeletal survey at the age of 2 years revealed hypoplasia of the second and terminal phalanges of the fifth digit, mild valgus shape of both acetabula and normal proportion of long bones (Figure 1k,l). Because of her low weight, reflux and low tolerance for oral food she was temporarily fed through a gastrostomy tube. The growth hormone production and full endocrine screening were normal. The total level of immunoglobulins and the subclasses screening were normal in two occasions; no AFP test was performed. She showed some improvement in her weight/height ratio, but the height continued to follow the −6 *SD*; therefore, tube feeding was discontinued (Figure 1h–j). During follow-up examinations, delay in speech and in motoric functions was noted. At the age of 2 years, an auditory brainstem response test showed bilateral sensorineural hearing loss of 90 dB, for which she received hearing aids. Neurological evaluation was normal except for high-pitched voice and nasal speech, slightly brisk reflexes of the lower extremities and a slightly unstable straight-line walk which was not observed at later examinations. A brain MRI at the age of 13 years showed a narrow foramen magnum with mild herniation of the cerebellar tonsils (Figure 1g). EEG was normal. Because of complains of fatigue a cardiovascular examination was performed which lead to the identification of Wolff–Parkinson–White anomalies without supraventricular tachycardia. At the last examination at the age of 15 years, her height was 126.5 cm (−5.8 *SD*) and head circumference 48.3 cm (−3.9 *SD*). A prominent nose bridge with a long nose point, a sloping forehead, telecanthus, a short neck, and thoracic kyphosis were noted. Sexual development had been normal with normal puberty and development of secondary sexual characteristics. At age 15, her TIQ was estimated to be 85. She currently lives with her parents and attends a special school for children with hearing loss. No decline of intellectual or motor functions has been observed. She has good communication skills and neither had any severe or recurrent infections nor malignancies.

3.2 | Genetic analysis

Genomic microarrays revealed a normal female hybridization pattern and included several regions of homozygosity reflecting parental consanguinity. Exome sequencing did not identify homozygous or compound heterozygous variants in any of the OMIM-referenced genes associated with autosomal recessive isolated or syndromic forms of primary microcephaly. Therefore, we subsequently filtered WES data for rare (minor allele frequency [MAF] <0.5% in the 1,000 Genomes database and the Exome Variant Server (EVS; NHLBI Exome Sequencing Project [ESP])), homozygous (allele frequency ≥75%) variants. Among the variants identified, only one variant was predicted to have a severe impact of protein function. In Exon 15 of *RAD50*, we identified homozygosity for the alteration c.2524G > A located at the last base of this exon and predicted to disrupt the adjacent donor splice splice site. This variant was embedded within the largest homozygous stretch of 22.6 Mb on chromosome 5q which was identified in this

patient based on the WES data. Both parents were heterozygous carriers for the identified c.2524G > A variant in *RAD50* which was neither annotated as a common single nucleotide polymorphism, nor found in >13,000 exomes within the EVS (National Heart, Lung, and Blood Institute ESP, Seattle, WA). This variant was identified with a MAF of 1.072e-4 in the gnomAD database (access date July 10, 2019), but only in the heterozygous state. As the c.2524G > A variant affects the last base of exon 15 and was predicted to disrupt the adjacent donor splice site, we analyzed the effect of this variant on splicing of *RAD50* mRNA, isolated from skin fibroblasts derived of the index patient, by RT-PCR and subsequent Sanger sequencing. We could show that the c.2524G > A variant leads to a major transcript that is generated by complete skipping of exon 15 of *RAD50*, therefore predicted to induce a frameshift and premature protein truncation (RAD50 p.Met800Phefs*7) (Figure 2a). Additionally, we observed a correctly spliced minor transcript variant carrying the p.Val842Ala amino acid substitution predicted from the c.2524G > A missense variant.

3.3 | Radioresistant DNA synthesis

Considering that RAD50 forms a complex with NBS and MRE11 which then recruits ATM at the sites of DSBs, we tested whether downregulation of DNA synthesis normally occurring after gamma irradiation was intact in cells harboring the *RAD50* mutation, or if this process is suppressed, as observed in cells lacking ATM. Exposure of wild-type fibroblasts to radiation halted DNA synthesis in these cells as shown in Figure 2b as percentage relative to DNA synthesis under no radiation. However, treatment of skin fibroblasts derived from our proband lead to radioresistant DNA synthesis almost similar to fibroblasts derived from an individual with AT indicating that, similarly to a

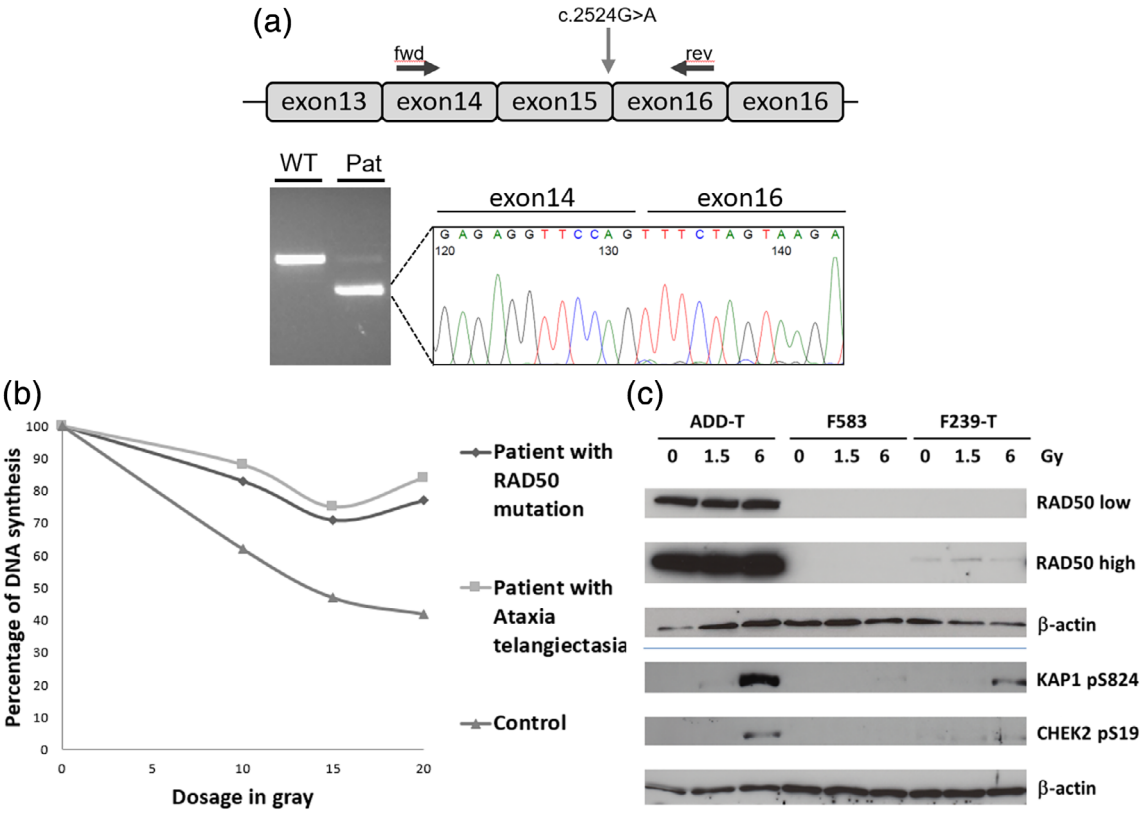

FIGURE 2 Genetic analysis, DNA synthesis, and ataxia telangiectasia-mutated (ATM) signaling. (a) RT-PCR analysis of *RAD50*. Schematic representation of the amplified region of *RAD50* cDNA and locations of primers used for the amplification (upper panel). The black arrow indicates the position of the primers used for amplification, the gray arrow indicated the position of the c.2524G > A mutation in exon 15. RT-PCR analysis of *RAD50* in the patient showed two different transcripts: one alternative transcripts of smaller size, and one transcript of corresponding size compared to WT (lower panel). Sequencing of the smaller RT-PCR products derived from patient cDNA revealed that the c.2524G > A mutation mainly resulted in a splicing product characterized by exon 15 skipping inducing a frameshift and premature protein truncation (RAD50 p.Met800Phefs*7). (b) DNA synthesis after exposure to γ-radiation in fibroblasts of our patient (lozenge symbol), a patient with ataxia telangiectasia (square), and control individual (triangle) as percentage of DNA synthesis at no exposure to radiation. (c) Whole cell protein lysates of fibroblasts from a healthy donor (ADD-T), from the patient described in this study (F583) and from the previously reported patient with RAD50 deficiency (F239-T) were comparatively assessed for RAD50 protein levels (upper panel) and for the radiation-induced phosphorylation of the ATM targets CHEK2 (pSer19) and KAP1 (pSer824) (lower panel). Cells had been irradiated with 0, 1.5, or 6 Gy as indicated, and proteins had been extracted at 30 min after irradiation. RAD50 immunoreactivity is shown at different exposure times (labeled as "low" and "high"). β-actin served as a loading control [Color figure can be viewed at wileyonlinelibrary.com]

mutation in ATM, the identified c.2524G > A variant in *RAD50* induces radioresistant DNA synthesis.

3.4 | RAD50 protein levels and ATM signaling

The effects of the c.2524G > A variant on RAD50 protein levels and on radiation-induced ATM signaling were further investigated by immunoblotting after irradiation of the fibroblasts with 0, 1.5, or 6 Gy (Figure 2c). RAD50 protein was almost undetectable in the F583 fibroblasts, even after long exposure times at which fibroblasts from the previously reported RAD50-deficient patient (F239-T) showed traces of RAD50 protein. We additionally assessed the levels of the other two MRN complex members, MRE11A and NBN, and found a strong reduction for both these proteins that was even more pronounced in the F583 fibroblasts than in F239-T cells (Figure S1). Similarly, the phosphorylation of the known ATM kinase targets CHEK2 and KAP1 was absent at 1.5 Gy and was barely detectable at 6 Gy of irradiation which was consistent with a marked deficiency in radiation-induced DNA damage signaling (Figure 2c).

4 | DISCUSSION

We report a girl of Turkish descent with a distinct phenotype carrying a novel homozygous variant in the *RAD50* gene. This variant, c.2524G > A in exon 15 of *RAD50*, affects the last base at exon 15 and we could show that it disrupts the adjacent donor splice site inducing skipping of this exon and resulting in a frameshift, premature protein truncation and most likely, loss of RAD50 function.

To date, only one individual with biallelic *RAD50* mutations has been reported (Barbi et al., 1991; Waltes et al., 2009). A comparison of the features of our patient, the previously reported patient and patients with NBS is summarized in Table 1. Both RAD50 subjects were small for gestational age and microcephalic at birth, had similar dysmorphic facial features, postnatal short stature, and progressive microcephaly. Both individuals had normal sexual development, no hormonal deficiencies, mild learning disability, and no decline in intellect, or psychomotor functions. Cultured fibroblasts from both individuals displayed abnormal radioresistant DNA synthesis after gamma-radiation and severe reduction of RAD50 protein on immunoblots. Evidence of spontaneous chromosome instability was observed in the first reported individual, but the karyotype and genomic copy number in leukocytes of our patient were normal. Both girls show no sign of immunodeficiency or recurrent infections, which are associated with NBS and also with the NBS-like disorders, NHEJ1 deficiency, and LIG4 deficiency (Altmann & Gennery, 2016; Dutrannoy et al., 2010; Varon et al., 1993). At the time of writing, no malignancies are reported.

Human *RAD50* deficiency belongs to the spectrum of MRN-related disorders. This clinical continuum also includes NBS and ATLD Type 1. Based on the clinical characterization of the index patient described herein and the comparison with the previously reported patient, we are now able to determine distinctive phenotype features resulting from *RAD50* mutations. Compared to ATLD Type 1, individuals with *RAD50* mutations do not present with strong neurological signs or symptoms, nor signs of neurodegeneration and with only mild learning disabilities.

ATLD Type 1 is caused by mutations in *MRE11A* and it has been associated with progressive cerebellar ataxia. However, biallelic *MRE11A* mutations have also been reported in two unrelated individuals sharing severe primary microcephaly, moderate to severe intellectual disability and pyramidal signs, but no cerebellar atrophy, nor immunodeficiency (Matsumoto et al., 2011). The authors define this disorder as a Nijmegen breakage-like syndrome. Similarly, *RAD50* mutations have also been classified as causing a Nijmegen breakage-like syndrome, and indeed, there is phenotypical overlap to individuals with *NBS* (Varon et al., 1993). We also note that the segregation pattern in this family, including heterozygous parents and one niece identified with a diagnosis of Seckel syndrome, is supportive of an autosomal recessive microcephaly syndrome (Figure 1m).

Still, the main difference between RAD50-related syndrome and "classic" NBS caused by *NBN* mutations is the absence of reported sensitivity to infections and increased risk of malignancies (Varon et al., 1993). Commonalities are mostly in the severe growth retardation already present in utero, the congenital microcephaly, the mild/moderate ID, and global similar dysmorphism. However, in most cases of NBS, there is a progressive microcephaly and a progressive growth improvement, leading to more evident disproportion with increasing age. This type of progression does not seem to apply for the patient with *RAD50* mutations in our study. Thus, although this syndrome does represent a NBS-like disorder, we prefer the name of RAD50 deficiency to account for these clinical differences and to distinguish it from other NBS-like disorders.

Waltes et al. also reported a heterozygous state for the rare variant c.506G > A, p.Arg169His (rs776134250), in NBN in their individual with biallelic RAD50 mutations. In the patient described here, no such NBN variant was detected in the exome sequencing, confirming that the clinical phenotype essentially results from the RAD50 mutation. This also implies that the observed instability of the partner proteins in the MRN complex, MRE11A and NBN, results from the RAD50 deficiency. A similar destabilization of all three members of the MRN complex has been reported in ATLD Type 1 patients (Delia et al., 2004; Fievet et al., 2019; Stewart et al., 1999). It is possible that the residual levels of these three proteins to some degree modulate the clinical phenotype in a tissue-specific manner.

An increasing number of children are presumably going to be diagnosed through whole-exome sequencing, meanwhile no management guidelines exist for RAD50-related disorder. Currently, it is unknown if patients with *RAD50* mutation have an increased risk of developing malignancies. However, two cases of colon carcinoma and one case of lung carcinoma were found within the family of our index patient (Figure 1m). Therefore, it is advisable to manage individuals with the RAD50-related disorder similarly to NBS individuals, as we cannot exclude that also *RAD50* mutation increases the risk of malignancies. We recommend, after initial diagnosis, consultation of a

TABLE 1 Overview of clinical and genetic features RAD50-related syndrome and NBS

	Individual 1 (Barbi et al., 1991; Waltes et al., 2009)	Individual 2 (this report)	NBS (Chrzanowska et al., 1995; Nijmegen breakage syndrome, 2000; Varon et al., 1993)
Sex	Female	Female	Both
Ethnicity	German	Turkish	Mostly associated with western Slavic
Age	23[a]	15[a]	
Mutation	c.3277C → T c.3939A → T	Homozygous c.2524G > A	Inactivating variants in *NBN* (Nibrin), most common c.657-661del5
Protein change and expression level	p.(Arg1093*) and p.X1313TyrextX*66	p.(Met800Phefs*7) and low-level p.(Val842Ile)	Several
Clinical manifestations			
Gestational age (weeks)	40	37	Normal
Birth weight (g)	1,835 (<−2.5 *SD*)	1,520 (<−3.5 *SD*)	<−2*SD* to normal
Birth head circumference (cm)	26.5 (<−6.5 *SD*)	29.5 (<−3.5 *SD*)	Microcephalic to normal
Birth body length (cm)	41 (<−4 *SD*)	36 (<−7.5 *SD*)	Often IUGR
Distinctive phenotype			
Sloping forehead	+	+	+
Broad nasal bridge	+	+	+
Prominent eyes	+	–	+
Epicanthal folds	+	–	Common
Widely spaced nipples	+	+	–
Hypoplastic nasal septum	+	+	+
Bilateral clinodactyly	+	+	Common
Brachydactyly	N. d.	+	–
Sandal gap	N. d.	+	Common
Cutaneous vascular anomalies	+	+	Occasionally
Hyperpigmentation and hypopigmentation	+	+	Common
Neurological symptoms			Very rare
Reflex	Normal	Normal	
High pitched voice	N. d.	+	
Hyperopia	+	–	
Sensorineural hearing loss	N. d.	+	
Ataxia	Subtle unstable straight-line walk	–	–
Immunology			
Recurrent infections	–	–	+
Ig status	Normal	Normal	Low IgG and IgA
Lymphocyte counts	Normal	Normal	Low T cells
Cellular features			
Chromosome instability	+	(normal karyotype)	+
Radioresistant DNA synthesis	+	+	+
Clinical manifestations			
Age	23 years	15 years	
Height (cm)	130 (<−4.5 *SD*)	126.5 (<−5 *SD*)	Growth retardation
Weight (kg)	29 (<−3 *SD*)	25.3 (<−3.5 *SD*)	Growth retardation
Head circumference (cm)	43 (−10 *SD*)	48.3 (<−5 *SD*)	Microcephaly
NBS-like facial features	+	+	+

TABLE 1 (Continued)

	Individual 1 (Barbi et al., 1991; Waltes et al., 2009)	Individual 2 (this report)	NBS (Chrzanowska et al., 1995; Nijmegen breakage syndrome, 2000; Varon et al., 1993)
Sexual development	Normal	Normal	Premature ovarian failure
Intellectual disability	Mild to moderate	Borderline	Moderate to borderline
Malignancies	–	–	↑ risk (40% at the age of 20 years)

Note: The significance of "a" refers to age at the time of writing.
Abbreviations: IUGR, intrauterine growth retardation; NBS, Nijmegen breakage syndrome.

clinical geneticist, assessment of growth, immunologic state, and cognitive development. As applied in other syndromes associated with primordial dwarfism, overfeeding should be avoided and growth hormone supplementation should only be restricted to cases with proven GH deficiency. Puberty and development of secondary sexual characteristics should be carefully monitored and if needed, endocrine evaluation and pelvic ultrasound should be performed. Because of abnormal radioresistant DNA synthesis, we would advise against repeated radiographs or CT scan and instead suggest using diagnostic MRI or ultrasound where consistent with the medical indication. Clearly, further research and identification of more patients will be required to guide the clinical management of RAD50 deficiency.

5 | CONCLUSION

We report a second individual with biallelic *RAD50* mutation confirming the association of RAD50 dysfunction with a distinctive phenotype. Based on our patient and the previously reported case, RAD50 deficiency should be considered as a separate disease entity, within the MRN-related disorders, with facial features resembling NBS, that is, severe prenatal growth retardation and persistent postnatal growth restriction, congenital microcephaly, mild to borderline intellectual disability, normal sexual development, radioresistant DNA synthesis, and no immunodeficiency or myelodysplasia or early neurodegeneration as key features. We encourage description of additional cases to delineate adequate management advice.

ACKNOWLEDGMENTS

The authors thank our proband and her family for their collaboration in this study. The authors thank Marianne Doornbos for patient care and Detlev Schindler for his seminal contribution of fibroblast cell lines. G. M. S. M. is supported by the ZonMW Top grant # 91217045.

CONFLICT OF INTEREST

The authors declare no conflict of interest.

AUTHOR CONTRIBUTIONS

Aviël Ragamin took the lead in writing the manuscript under supervision of Grazia M. S. Mancini and input of all authors. Gökhan Yigit, Kristine Bousset, Tim M. Strom, Thilo Dörk, and Bernd Wollnik performed the genetic analysis and immunoblotting. Frans W. Verheijen performed the DNA synthesis under radiation experiments. Marie-Claire Y. de Wit and Grazia M. S. Mancini provided clinical consult and interpretation. Thilo Dörk, Bernd Wollnik, and Grazia M. S. Mancini helped supervise the project. All authors commented on the draft and approved the final manuscript. Aviël Ragamin and Gökhan Yigit contributed equally to the manuscript.

DATA AVAILABILITY STATEMENT

The data that support the findings of this study are available on request from the corresponding author. The genomic data are not publicly available due to privacy or ethical restrictions.

ORCID

Grazia M. S. Mancini https://orcid.org/0000-0002-1211-9979

REFERENCES

Altmann, T., & Gennery, A. R. (2016). DNA ligase IV syndrome; a review. *Orphanet Journal of Rare Diseases*, *11*(1), 137.

Aparicio, T., Baer, R., & Gautier, J. (2014). DNA double-strand break repair pathway choice and cancer. *DNA Repair (Amst)*, *19*, 169–175.

Barbi, G., Scheres, J. M., Schindler, D., Taalman, R. D., Rodens, K., Mehnert, K., … Seyschab, H. (1991). Chromosome instability and X-ray hypersensitivity in a microcephalic and growth-retarded child. *American Journal of Medical Genetics*, *40*(1), 44–50.

Bogershausen, N., Tsai, I. C., Pohl, E., Kiper, P. O., Beleggia, F., Percin, E. F., … Wollnik, B. (2015). RAP1-mediated MEK/ERK pathway defects in Kabuki syndrome. *The Journal of Clinical Investigation*, *125*(9), 3585–3599.

Chamankhah, M., & Xiao, W. (1999). Formation of the yeast Mre11-Rad50-Xrs2 complex is correlated with DNA repair and telomere maintenance. *Nucleic Acids Research*, *27*(10), 2072–2079.

Chatterjee, N., & Walker, G. C. (2017). Mechanisms of DNA damage, repair, and mutagenesis. *Environmental and Molecular Mutagenesis*, *58*(5), 235–263.

Chrzanowska, K. H., Kleijer, W. J., Krajewska-Walasek, M., Bialecka, M., Gutkowska, A., Goryluk-Kozakiewicz, B., et al. (1995). Eleven polish patients with microcephaly, immunodeficiency, and chromosomal instability: The Nijmegen breakage syndrome. *American Journal of Medical Genetics*, *57*(3), 462–471.

de Wit, J., Jaspers, N. G., & Bootsma, D. (1981). The rate of DNA synthesis in normal human and ataxia telangiectasia cells after exposure to X-irradiation. *Mutation Research*, *80*(1), 221–226.

Delia, D., Piane, M., Buscemi, G., Savio, C., Palmeri, S., Lulli, P., … Chessa, L. (2004). MRE11 mutations and impaired ATM-dependent responses in

an Italian family with ataxia-telangiectasia-like disorder. *Human Molecular Genetics*, *13*(18), 2155–2163.

Dutrannoy, V., Demuth, I., Baumann, U., Schindler, D., Konrat, K., Neitzel, H., … Varon, R. (2010). Clinical variability and novel mutations in the NHEJ1 gene in patients with a Nijmegen breakage syndrome-like phenotype. *Human Mutation*, *31*(9), 1059–1068.

Fernet, M., Gribaa, M., Salih, M. A., Seidahmed, M. Z., Hall, J., & Koenig, M. (2005). Identification and functional consequences of a novel MRE11 mutation affecting 10 Saudi Arabian patients with the ataxia telangiectasia-like disorder. *Human Molecular Genetics*, *14*(2), 307–318.

Fievet, A., Bellanger, D., Valence, S., Mobuchon, L., Afenjar, A., Giuliano, F., … Stern, M. H. (2019). Three new cases of ataxia-telangiectasia-like disorder: No impairment of the ATM pathway, but S-phase checkpoint defect. *Human Mutation*, *40*(10), 1690–1699.

Hoa, N. N., Shimizu, T., Zhou, Z. W., Wang, Z. Q., Deshpande, R. A., Paull, T. T., … Sasanuma, H. (2016). Mre11 is essential for the removal of lethal topoisomerase 2 covalent cleavage complexes. *Molecular Cell*, *64*(5), 1010.

Kobayashi, J., Antoccia, A., Tauchi, H., Matsuura, S., & Komatsu, K. (2004). NBS1 and its functional role in the DNA damage response. *DNA Repair (Amst)*, *3*(8–9), 855–861.

Lavin, M. F., Kozlov, S., Gatei, M., & Kijas, A. W. (2015). ATM-dependent phosphorylation of all three members of the MRN complex: From sensor to adaptor. *Biomolecules*, *5*(4), 2877–2902.

Luo, G., Yao, M. S., Bender, C. F., Mills, M., Bladl, A. R., Bradley, A., & Petrini, J. H. (1999). Disruption of mRad50 causes embryonic stem cell lethality, abnormal embryonic development, and sensitivity to ionizing radiation. *Proceedings of the National Academy of Sciences of the United States of America*, *96*(13), 7376–7381.

Matsumoto, Y., Miyamoto, T., Sakamoto, H., Izumi, H., Nakazawa, Y., Ogi, T., … Matsuura, S. (2011). Two unrelated patients with MRE11A mutations and Nijmegen breakage syndrome-like severe microcephaly. *DNA Repair (Amst)*, *10*(3), 314–321.

Mehta, A., & Haber, J. E. (2014). Sources of DNA double-strand breaks and models of recombinational DNA repair. *Cold Spring Harbor Perspectives in Biology*, *6*(9), a016428.

Palmeri, S., Rufa, A., Pucci, B., Santarnecchi, E., Malandrini, A., Stromillo, M. L., … Federico, A. (2013). Clinical course of two Italian siblings with ataxia-telangiectasia-like disorder. *Cerebellum*, *12*(4), 596–599.

Pietrucha, B., Heropolitanska-Pliszka, E., Geffers, R., Enssen, J., Wieland, B., Bogdanova, N. V., & Dork, T. (2017). Clinical and biological manifestation of RNF168 deficiency in two polish siblings. *Frontiers in Immunology*, *8*, 1683.

Schroder-Heurich, B., Wieland, B., Lavin, M. F., Schindler, D., & Dork, T. (2014). Protective role of RAD50 on chromatin bridges during abnormal cytokinesis. *The FASEB Journal*, *28*(3), 1331–1341.

Stewart, G. S., Maser, R. S., Stankovic, T., Bressan, D. A., Kaplan, M. I., Jaspers, N. G., … Taylor, A. M. (1999). The DNA double-strand break repair gene hMRE11 is mutated in individuals with an ataxia-telangiectasia-like disorder. *Cell*, *99*(6), 577–587.

Stingele, J., Bellelli, R., & Boulton, S. J. (2017). Mechanisms of DNA-protein crosslink repair. *Nature Reviews. Molecular Cell Biology*, *18*(9), 563–573.

The International Nijmegen Breakage Syndrome Study Group. (2000). Nijmegen breakage syndrome. *Archives of Disease in Childhood*, *82*(5), 400–406.

van Zutven, L., Mancini, G. M. S., Bindels-de Heus, K., van den Akker, E. L. T., Hulsman, L. O. M., Smit, M., & Berna, B. H. (2018). Mixoploidy combined with aneuploidy in a 13 year-old patient with severe multiple congenital abnormalities and intellectual disability. *American Journal of Medical Genetics. Part A*, *176*(2), 492–495.

Vandervore, L. V., Schot, R., Kasteleijn, E., Oegema, R., Stouffs, K., Gheldof, A., … Mancini, G. M. S. (2019). Heterogeneous clinical phenotypes and cerebral malformations reflected by rotatin cellular dynamics. *Brain*, *142*(4), 867–884.

Varon, R., Demuth, I., Chrzanowska, K. H. (1993–2020). *Nijmegen breakage syndrome*. In: Adam MP, Ardinger HH, Pagon RA, Wallace SE, Bean LJH, Stephens K, Amemiya A. (Eds.). GeneReviews® [Internet]. Seattle, WA: University of Washington. [Last updated February 2, 2017]

Waltes, R., Kalb, R., Gatei, M., Kijas, A. W., Stumm, M., Sobeck, A., … Dork, T. (2009). Human RAD50 deficiency in a Nijmegen breakage syndrome-like disorder. *American Journal of Human Genetics*, *84*(5), 605–616.

Williams, G. J., Lees-Miller, S. P., & Tainer, J. A. (2010). Mre11-Rad50-Nbs1 conformations and the control of sensing, signaling, and effector responses at DNA double-strand breaks. *DNA Repair (Amst)*, *9*(12), 1299–1306.

Xiao, Y., & Weaver, D. T. (1997). Conditional gene targeted deletion by Cre recombinase demonstrates the requirement for the double-strand break repair Mre11 protein in murine embryonic stem cells. *Nucleic Acids Research*, *25*(15), 2985–2991.

Yang, Y. G., Saidi, A., Frappart, P. O., Min, W., Barrucand, C., Dumon-Jones, V., … Wang, Z. Q. (2006). Conditional deletion of Nbs1 in murine cells reveals its role in branching repair pathways of DNA double-strand breaks. *The EMBO Journal*, *25*(23), 5527–5538.

Zhu, J., Petersen, S., Tessarollo, L., & Nussenzweig, A. (2001). Targeted disruption of the Nijmegen breakage syndrome gene NBS1 leads to early embryonic lethality in mice. *Current Biology*, *11*(2), 105–109.

SUPPORTING INFORMATION

Additional supporting information may be found online in the Supporting Information section at the end of this article.

How to cite this article: Ragamin A, Yigit G, Bousset K, et al. Human *RAD50* deficiency: Confirmation of a distinctive phenotype. *Am J Med Genet Part A*. 2020;182A:1378–1386. https://doi.org/10.1002/ajmg.a.61570